Transition pressures and enthalpy barriers for the cubic diamond→β-tin transition in Si and Ge under nonhydrostatic conditions

Katalin Gaál-Nagy[1,2,*] and Dieter Strauch[2]
[1]*European Theoretical Spectroscopy Facility (ETSF), CNISM-CNR-INFM, and Dipartimento di Fisica dell'Università degli Studi di Milano, via Celoria 16, I-20133 Milano, Italy*
[2]*Institut für Theoretische Physik, Universität Regensburg, D-93040 Regensburg, Germany*
(Received 29 August 2005; revised manuscript received 21 February 2006; published 4 April 2006)

We present an *ab initio* study of the phase transition cubic diamond→β-tin in Si and Ge under hydrostatic and nonhydrostatic pressure. For this purpose we have developed a method to calculate the influence of nonhydrostatic pressure components not only on the transition pressure but also on the enthalpy barriers between the phases. The calculations were performed using the plane-wave pseudopotential approach to the density-functional theory within the local-density and the generalized-gradient approximation implemented in VASP. We find good agreement with available experimental and other theoretical data.

DOI: 10.1103/PhysRevB.73.134101 PACS number(s): 64.70.Kb, 71.15.Nc, 81.40.Vw

I. INTRODUCTION

The phase transitions in silicon (Si) and germanium (Ge) from the cubic-diamond (cd) phase (cubic-diamond structure) to the β-tin phase [body-centered tetragonal (bct) structure] are two of the most studied solid-solid phase transitions in condensed matter physics, both experimentally[1–23]and theoretically.[23–49]In the experiment, the phase transition in Si occurs at around 110 kbar and in Ge at around 105 kbar, where also lower values of the transition pressure are obtained. These lower values are often attributed to nonhydrostatic conditions, which are able to reduce the transition pressure.[13]

In fact, the pressure in the anvil cell is not exactly hydrostatic. Usually at pressures up to 100 kbar, the pressure-transmitting medium yields nearly hydrostatic conditions.[50] Above 150 kbar, a nonhydrostatic pressure profile is visible, and at very high pressures, the pressure-transmitting medium solidifies resulting in strong nonhydrostatic effects. Even in the hydrostatic pressure regime there is a small pressure gradient.[51] Nonhydrostatic pressure profiles can also be an effect of the geometry of the cell.[52] Because of relaxation phenomena that happen in the pressure-transmitting medium and/or in the crystal, the time for compressing and decompressing has an influence on the measurement.

In theoretical investigations, generally hydrostatic conditions are assumed. Within calculations using the local-density approximation (LDA), the calculated transition pressures vary between 70 and 99 kbar for Si and between 73 and 98 kbar for Ge. Usually, the transition pressure is strongly underestimated by LDA calculations, whereas calculations using the generalized-gradient approximation (GGA) match the experimental value better (102–164 kbar for Si and 96–118 kbar for Ge). In any case, the discrepancy between experimental and theoretical results can also be due to nonhydrostatic pressure conditions in the experiment. *Ab initio* calculations considering nonhydrostatic pressure are rare[53,54] and deal just with the transition pressure. The influence of nonhydrostatic conditions on the enthalpy barrier between the two phases is not studied within an *ab initio* calculation until now. Therefore, we developed a method for the extraction of the enthalpy from an energy surface to calculate the transition pressure as well as the enthalpy barriers also for nonhydrostatic conditions. In a first step, we obtain the transition pressure and the enthalpy barrier between both phases as a function of pressure starting from a numerical multiphase equation of state for hydrostatic conditions. Here a multiphase equation of state means a continuous, multivalued function $V(p)$, where V is the volume and p the pressure, similar to the one of the textbook example of the van der Waals gas. In a second step, this procedure is extended to nonhydrostatic conditions. All isotherms in this work are at 0 K.

This contribution is organized as follows: To begin with, we introduce the theoretical background of the method used here, namely, the multiphase equation of state (Sec. II). Then we apply this method to real systems, the cd→β-tin phase transition in Si and Ge. After mentioning the technical details of the total-energy calculation, we explain the procedure of calculating a multiphase equation of state from a given energy surface in case of hydrostatic and nonhydrostatic conditions (Sec. III). Finally, after a discussion of the results and comparison to available theoretical data (Sec. IV), we describe possible extensions of our procedure and summarize (Sec. V).

II. THEORY OF THE MULTIPHASE EQUATION OF STATE

In this section, we describe the theoretical background on which our method is based. Especially, we figure out the differences between hydrostatic and nonhydrostatic conditions.

A. Multiphase equation of state for hydrostatic conditions

Neglecting temperature and zero-point motion effects, the phase with the lowest enthalpy $H=E+pV$ is the stable one. Therefore, the transition pressure p^t for a first-order pressure-induced phase transition from the cd phase to the β-tin phase

can be determined from the crossing of the corresponding enthalpy curves $H^{\mathrm{cd}}(p)$ and $H^{\beta\text{-tin}}(p)$ with $H^{\mathrm{cd}}(p^{\mathrm{t}})=H^{\beta\text{-tin}}(p^{\mathrm{t}})$. First-order phase transitions are accompanied by a discontinuity ΔV in the volume and an overcoming of an enthalpy barrier, which is located between the phases and has a height of ΔH.

Under *hydrostatic* conditions the pressure is defined as $p=-\partial E/\partial V$. It can also be determined from the stress tensor $\boldsymbol{\sigma}$.[55,56] Since the structures here are orthogonal, the off-diagonal components of $\boldsymbol{\sigma}$ vanish, and $\boldsymbol{\sigma}$ has the form

$$\boldsymbol{\sigma}=\begin{pmatrix}\sigma_{11} & & \\ & \sigma_{22} & \\ & & \sigma_{33}\end{pmatrix}=\begin{pmatrix}-p_x & & \\ & -p_y & \\ & & -p_z\end{pmatrix}. \tag{1}$$

We are using a tetragonal cell, and thus $p_x=p_y$. Under *hydrostatic* conditions all three components are equal and correspond to the external pressure p,

$$p_x=p_y=p_z=p. \tag{2}$$

B. Multiphase equation of state for nonhydrostatic conditions

Under *nonhydrostatic* conditions, also the strain has to be taken into account. Similar to the stress tensor of Eq. (1), the strain tensor $\boldsymbol{\epsilon}$ can be reduced to a diagonal form for orthogonal systems[55–57]

$$\boldsymbol{\epsilon}=\begin{pmatrix}\epsilon_{11} & & \\ & \epsilon_{22} & \\ & & \epsilon_{33}\end{pmatrix}=\begin{pmatrix}\epsilon_x & & \\ & \epsilon_y & \\ & & \epsilon_z\end{pmatrix} \tag{3}$$

where ϵ_x, ϵ_y, and ϵ_z are along the Cartesian crystal axes. For small stress and homogeneous strain, the components of $\boldsymbol{\epsilon}$ can be derived as[55,57]

$$\epsilon_{jj}=\frac{x_j'-x_j}{x_j}, \tag{4}$$

where x_j is the lattice parameter in the j direction. Here x_j corresponds to the unstrained and x_j' to the strained crystal. Including stress and strain, the enthalpy density $\tilde{H}=H/V_0$ can be written as[57]

$$\tilde{H}=\tilde{E}-\sum_{j=1}^{3}\sigma_{jj}\epsilon_{jj}, \tag{5}$$

where $\tilde{E}=E/V_0$ is the density of the total energy, and V_0 is the equilibrium volume. With respect to the common formula for hydrostatic conditions $H=E+pV=E+p(V-V_0)+pV_0$, the last term $+pV_0$ is missing here.

Under *nonhydrostatic* conditions, we define the average pressure as

$$p_0=\tfrac{1}{3}(p_x+p_y+p_z)=-\tfrac{1}{3}\,\mathrm{tr}\boldsymbol{\sigma}, \tag{6}$$

which is again equal to the external pressure in the case of hydrostatic conditions.

The calculation of the enthalpy at nonhydrostatic stress is based on Eq. (5). The numerical realization is described in the Appendix.

III. METHOD FOR DETERMINING A MULTIPHASE EQUATION OF STATE

In this section, we elucidate how a numerical multiphase equation of state can be obtained from an energy surface. First, we describe the computational details for calculating the energy surface in the case of the cd→β-tin transitions (Sec. III A). After this, we extract a numerical multiphase equation of state from the energy surface in the case of hydrostatic conditions in order to explain first results and to show the reliability of the enthalpy extraction method (Sec. III B). Last, we extend our method in order to derive nonhydrostatic conditions (Sec. III C).

A. Technical details

We have carried out our calculations with the Vienna *ab initio* simulation package (VASP).[58–61] It is based on a plane-wave pseudopotential approach to the density-functional theory (DFT).[62,63] We have used ultrasoft Vanderbilt-type pseudopotentials[64] as supplied by Kresse and Hafner.[65] The exchange-correlation potential has been calculated within the GGA due to Perdew *et al.*[66] for Si and Ge and the LDA[67,68] for Si only. The forces on the atoms are derived from a generalized form[60,69] of the Hellmann-Feynman theorem,[70] including Pulay forces.[71] For the ultrasoft pseudopotentials, a kinetic-energy cutoff of 270 eV (410 eV) for Si (Ge) has been sufficient for convergence of the total energy and provides an error smaller than 0.5 kbar (0.2 kbar) for Si (Ge) to the pressure according to the Pulay stress.[71] The special-point summation required a $18\times18\times18$ $(24\times24\times24)$ mesh of Monkhorst-Pack points,[72] which amounts to 864 (1962) **k** points in the irreducible wedge of the Brillouin zone for Si (Ge). Since the β-tin phase is metallic, we have used a Methfessel-Paxton smearing[73] with a width of 0.2 eV and have also used it for the cd phase, since it is not *a priori* clear whether a given set of volume V and ratio c/a of lattice constants yields a metallic or a semiconducting phase.

In order to minimize an energy offset between the structures, it is important to describe the structures of both phases within the same bct cell (lattice constants $a=b\neq c$) with two atoms in the basis at $(0,0,0)$ and $(0,0.5a,0.25c)$. The symmetry of the cd phase requires $c/a=\sqrt{2}$, whereas c/a can vary for the β-tin phase. Using the bct cell, the structure of the cd phase with respect to the conventional face-centered-cubic cell is rotated by 45° around the c axis. In the following, CD and BCT denote the structure of the cd- and the β-tin phase using the bct cell.

B. Applications to hydrostatic conditions

We have calculated the total energy as a function of V and c/a. The corresponding energy surface $E(V,c/a)$ is shown in Fig. 1 for Si using the GGA (similar results are obtained for Ge within GGA and for Si within LDA). The two local energy minima, related to the two phase equilibria, with a saddle in between, are visible. The pressure $p_0(V,c/a)$ as obtained from Eqs. (1) and (6) is included in the figure. Except along the (dotted) hydrostatic line with $p_x=p_z$, the pressure is nonhydrostatic. The local minima are at the cross-

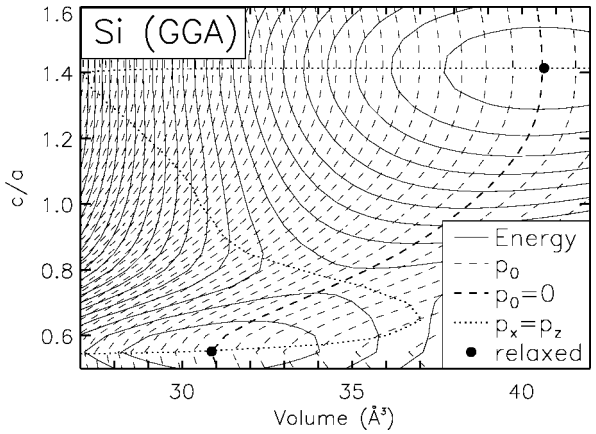

FIG. 1. Contour plot of the total energy $E(V,c/a)$ (solid lines) and of the average pressure $p_0(V,c/a)$ [dashed lines, see Eq. (6)] for Si with GGA. The bold-dashed line corresponds to the value $p_0=0$. The interval of the contour lines is 50 meV for the energy and 20 kbar for the pressure surfaces. The black dots mark the equilibrium positions of the cd ($c/a=\sqrt{2}$) and the β-tin phase ($c/a=0.55$). The dotted line marks the parameters under hydrostatic condition.

ing of the $p_0=0$ and the hydrostatic $p_x=p_z$ lines, which defines the equilibrium position. A similar graph can also be drawn for the enthalpy.[46]

Along the hydrostatic $p_x=p_z$ line, the structures are in a local equilibrium, meaning that the sum of internal and external forces caused by the pressure is zero. Hence, this condition can be used to extract the total energy E, the external pressure $p_0=p$, and the volume V from Fig. 1 in order to derive a multiphase equation of state $V(p)$. These curves are shown in Fig. 2. Here, $H(p)$ for the cd-and the β-tin phase (solid and dashed lines in Fig. 2) and, furthermore, the values along the line across the saddle (dotted line in Fig. 2) are accessible. The ideal cd structure ($c/a=\sqrt{2}$) has been reached

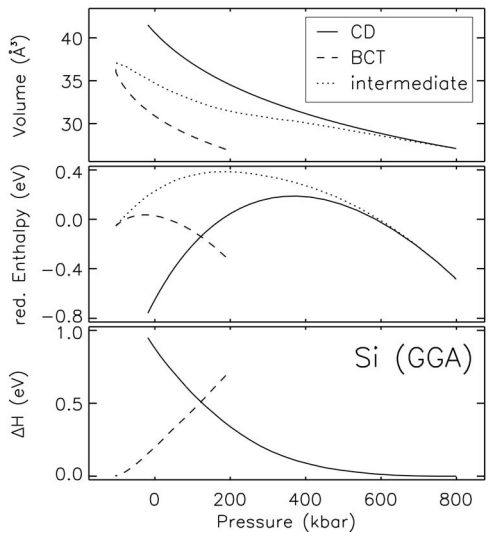

FIG. 2. Volume V, reduced enthalpy (see text), and enthalpy barrier ΔH as a function of the hydrostatic pressure for Si within GGA. The crossing of the solid and dashed lines determines the transition pressure.

TABLE I. Transition pressures p^t, volume changes ΔV, and enthalpy barriers ΔH derived from the multiphase equation of state in comparison to our previous results obtained with an alternative method (in parenthesis).[46]

	Ge-GGA	Si-GGA	Si-LDA
p^t (kbar)	96 (96)	122 (121)	80 (79)
ΔV(Å^3)	7.5 (7.5)	8.3 (8.3)	8.5 (8.5)
ΔH (meV)	421 (423)	510 (515)	502 (508)

only within an error of 1% for the lattice-parameter ratio. In order to discriminate the enthalpy curves against each other and to enhance the visibility we have subtracted a linear baseline (reduced enthalpy). The local stability is in accordance with the fact that the $V(p)$ curves are monotonically decreasing and the $H(p)$ curves are convex. This is in contrast to the textbook example, the van der Waals gas, where the line corresponding to the dotted line of $H(p)$ is concave and signals local instability.

The transition pressure p^t obtained from the crossing of the enthalpy curves are listed in Table I. The corresponding change ΔV in the volume at the phase transition can be read from the upper panel of Fig. 2 as the difference between $V^{cd}(p^t)$ (solid line) and $V^{\beta\text{-tin}}(p^t)$ (dashed line). Analogously, the enthalpy barrier ΔH can be determined from the figures. In order to check the reliability of this method, we compare the results to our previous ones[46] based on the same total-energy calculations but obtained with a different method to evaluate the transitions pressures and enthalpy barriers. The agreement is very good, and the small differences are due to numerical errors. Thus, we can trust in the enthalpy extraction method developed here.

Since we have determined a multiphase equation of state, we can calculate also the enthalpy barrier as a function of pressure. We have to distinguish between the barrier for the cd$\rightarrow\beta$-tin transition, approaching from the cd phase, and the one for the β-tin$\rightarrow$cd transition, approaching from the β-tin phase. In general, the enthalpy barrier ΔH has its origin in the energy saddle between the two phases. It can be calculated as the difference of the enthalpy of the phases and the one from the saddle. The corresponding curves are shown in the middle panel of Fig. 2. In particular, for the cd$\rightarrow\beta$-tin transition the enthalpy barrier is the difference between the enthalpy of the cd phase (solid line) and the one of the saddle (dotted line). Likewise, for the β-tin$\rightarrow$cd transition it is the difference between the enthalpy of the β-tin phase (dashed line) and the saddle (dotted line). The resulting enthalpy barriers approaching from the cd- and the β-tin phase are shown in the lower panel of Fig. 2. At the transition pressure p^t, the enthalpy barriers from both phases have the same height. The determination of the enthalpy barrier as a function of pressure is important to estimate the barrier in the case of over- or underpressurizing the medium. Hence, the phase transitions will happen at a pressure different from p^t, which results in a different height of the barrier. As expected, the enthalpy barrier from the cd phase is decreasing with increasing pressure, whereas the one from the β-tin phase decreases with decreasing pressure. At zero pressure, there is

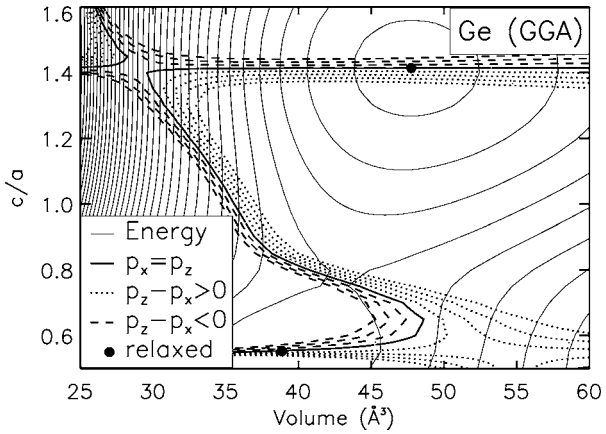

FIG. 3. Contour plot of the total energy $E(V,c/a)$ (solid lines) for Ge (GGA) with an interval of 0.2 eV between contour lines. Besides the hydrostatic condition (bold solid line) nonhydrostatic conditions ($p_z-p_x=-15,-10,\ldots,20$) are shown.

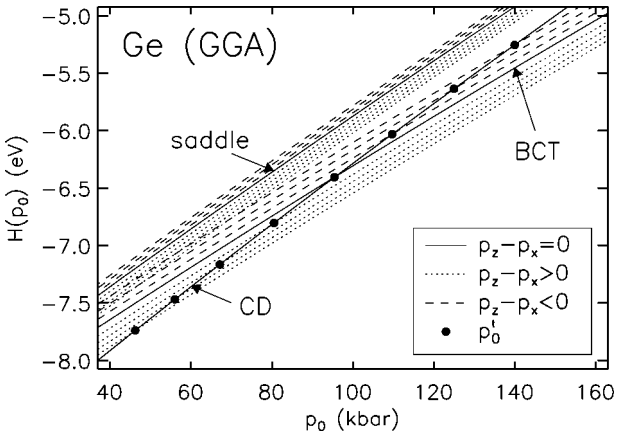

FIG. 4. Equation of state $H(p_0)$ for nonhydrostatic conditions as a function of the average pressure p_0. The difference p_z-p_x of two neighboring lines is 5 kbar. The black dots mark the transition pressures p_0^t.

still an enthalpy barrier left for the β-tin→cd transition. This points to the fact that there is no spontaneous transition β-tin →cd. In the experiment, the phase transition cd→β-tin is irreversible.

C. Applications to nonhydrostatic conditions

The procedure for determining transition pressures and enthalpy barriers described in Sec. III B can be extended to the case of nonhydrostatic pressure. Besides the hydrostatic condition $p_z-p_x=0$, the values for nonhydrostatic pressure components $p_z-p_x=d\neq 0$ (with a fixed value of d) can be extracted from the energy surface $E(V,c/a)$ along the corresponding lines of Fig. 3. A first naive trial considering just the total energy E^{nh} under nonhydrostatic conditions and the corresponding values p_0^{nh} for the average pressure and V^{nh} for the volume gives wrong results, e.g., an increase of the transition pressure for $p_z>p_x$ and $p_z<p_x$. This is in contrast to the experimental observations. Thus, it is necessary to include nonisotropic strain in the calculation.

In the following, "the strain-only contribution" will be referred to as the difference between the enthalpy calculated with Eq. (5) and the enthalpy obtained by $H^{nh}=E^{nh}+p_0^{nh}V^{nh}$. From our numerical results it turns out that the strain-only contribution to the enthalpy is negligibly small for the cd phase; it is linear in the pressure for the β-tin phase, and it is nonlinear for the contribution along the line across the saddle. This effect is apparent in Fig. 4, where the enthalpy including strain is presented. Since the strain-only contribution to the enthalpy of the cd phase is nearly two orders of magnitude smaller than the one of the β-tin phase, the change of the transition pressure with respect to nonhydrostatic conditions is mainly due to the strain-only contribution to the β-tin phase. From Fig. 4 we can find the transition pressures for fixed nonhydrostatic conditions in the same manner as mentioned in Sec. III B.

In addition to the average transition pressure p_0^t, their components p_x^t and p_z^t in the x and z directions are also shown, as well as the enthalpy barrier at the phase transition as a function of p_z-p_x in Fig. 5. For the transition pressure, one has the relation $p_0^t=(2p_x^t+p_z^t)/3$. The boundary for the lowest pressure is fixed by the condition that the components of p_0 are not negative, since we exclude stretching the crystal. We find a strong lowering of the transition pressure if the pressure in the z direction is larger than in the x and y directions. Thus, the crystal is more stable against compression along the x- and y axes in the case of a strong nonhydrostatic component in these directions, which causes an increase of the transition pressure. The corresponding enthalpy barriers are lowering in any case, but their value remains still larger than the thermal energy at room temperature (RT).

Besides the nonhydrostatic effects, we can also finally consider the case of over- and underpressurization of the crystal. To this end, calculations of the enthalpy barriers as a function of the average pressure and nonhydrostatic conditions have been carried out (Fig. 6). At very high pressures and very large nonhydrostatic components, the enthalpy bar-

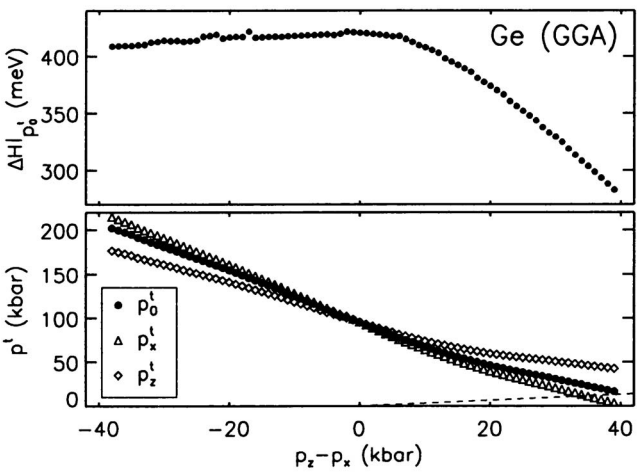

FIG. 5. Enthalpy barriers at the average transition pressures p_0^t and transition pressures (average transition pressure p_0^t and the corresponding components p_x^t and p_z^t) as a function of p_z-p_x. The dashed line marks the boundary $p_x=0$ and $p_z=0$.

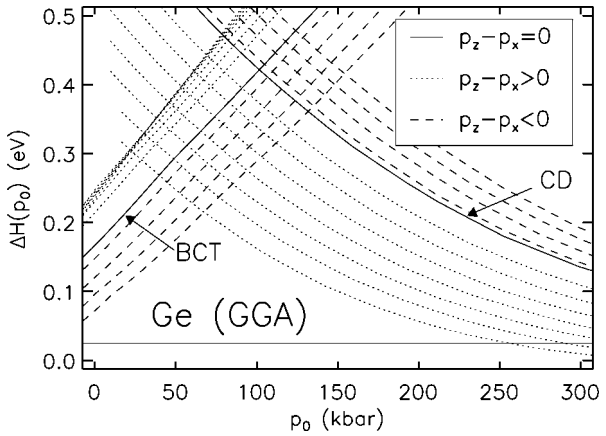

FIG. 6. Enthalpy barriers, as in Fig. 2, for fixed nonhydrostatic conditions $p_z-p_x=-20,-15,\ldots,$ 35 kbar. The solid horizontal line at 25 meV marks the thermal excitation energy at RT.

rier for the cd→β-tin transition is smaller than the thermal energy at RT, but these conditions do not appear by chance in the experiment; instead, they have to be applied by intention. In contrast, the enthalpy barrier is never smaller than 25 meV for the β-tin→cd transition even at the largest nonhydrostatic components with p_x, p_y, and p_z not negative (no stretching).

IV. DISCUSSION OF THE RESULTS

In the past, nonhydrostatic conditions have been investigated for different reasons.[53,54,74–78] Wang *et al.*[75,76] have worked on integrals exploring the work of pressure on a system, but their main goal was the investigation of stability criteria by examining the stiffness tensor. Libotte and Gaspard[77] already have included nonhydrostatic pressure in their work by a parameter within the work integral. Unfortunately, in their calculation using a semi-empirical tight-binding model they considered just the phase transition from the β-tin to the *Imma* phase, which appears by pressing the β-tin phase. Durandurdu[78] has considered the cd→β-tin transition under nonhydrostatic pressure in his molecular-dynamics study, but in fact, he assumed the pressure along just one direction with the other pressure components set to zero. However, this condition is not given in a diamond-anvil cell, which was the motivation of our work. Even if similar results are easily accessible from our data in order to compare to his, such a study is beyond our scope. Hence, directly comparable to our results are just the ones from Lee *et al.*[74] and Cheng *et al.*[53] Cheng.[54] Besides the transition pressures, the function $p_z^t(p_x^t)=ap_x^t+b$ is also given in these contributions. This function can be obtained from our results by a linear fit of the values for the transition pressure in Fig. 5. The additive constant corresponds to the lowest possible transition pressure. The results are summarized in Table II together with those of the references mentioned above.

Already Lee *et al.*[74] found a linear relation between p_z^t and p_x^t. But their results obtained by a molecular-dynamics (MD) investigation differ from those of Cheng *et al.*[53] and Cheng[54] which have also been obtained with VASP using GGA. Although our results have also been performed with VASP, their results for the transition pressure are slightly different from ours. This can be due to the fact that they have used different cells for the phases and also different pseudopotentials and convergence parameters. The choice of different unit cells can lead to an energy offset between the energy curves to which the transition pressure is very sensitive in the present case. Nevertheless, our results for the linear functions agree very well with those of Refs. 53 and 54. The difference of the additive constants rely on the different values of the transition pressures in the hydrostatic case. Since Cheng *et al.*[53] and Cheng[54] restricted themselves to the enthalpy difference between the phases using path integrals, the enthalpy barrier was not accessible to them.

TABLE II. Transition pressures p^t and linear relations of their components $p_z^t=ap_x^t+b$.

	Method	p^t (kbar)	$p_z^t=ap_x^t+b$ (kbar)	Reference
Si	LDA	79.6	$p_z^t=0.619p_x^t+29.8$	This work
Si	GGA	122.1	$p_z^t=0.606p_x^t+47.3$	This work
Si	GGA	114	$p_z^t=0.658p_x^t+39$	Cheng *et al.*[53] Cheng[54]
Si	MD	127	$p_z^t=p_x^t+90$	Lee *et al.*[74]
Ge	GGA	95.9	$p_z^t=0.651p_x^t+35.1$	This work
Ge	GGA	95	$p_z^t=0.737p_x^t+25$	Cheng *et al.*,[53] Cheng[54]

The experimental values for the transition pressures vary between 103 and 133 kbar for Si[1–7] and between 103 and 110 kbar for Ge[5–11] where the generally accepted values are at around 110 kbar and 105 kbar, respectively. In both cases, our results obtained with GGA agree perfectly, whereas the LDA result underestimates the experimental value, which is a well-known problem.

The good agreement of our results with the ones of Cheng *et al.*[53] and Cheng[54] confirm the reliability of our method, which provides a larger field of application. In addition, our method can be extended to, e.g., the β-tin→*Imma*→sh transitions in Si and Ge. After the extraction of a two-dimensional energy surface from a three-dimensional one using the values along the lines where two components of the stress tensor are equal (as in our previous work,[46,79]) the method mentioned here can be applied to this extracted surface. By the choice of two equal components, the main pressure direction is chosen. Further extensions even to non-orthorhombic structures are also possible.

V. SUMMARY

We have developed a method to investigate first-order high-pressure phase transitions. This method is based on the numerical determination of a multiphase equation of state, where the corresponding values are extracted from the total energy as a function of the volume and the ratio of the lattice constant with respect to pressure conditions. Besides the transition pressure and the volume change, which are also available with the common-tangent construction, the en-

thalpy barrier between the phases can be obtained with our method. A comparison to results for Si and Ge from common methods shows the reliability of the enthalpy extraction method. Furthermore, the enthalpy barrier can be determined as a function of the external pressure, which makes effects from over- and underpressurizing accessible. An extension of this method also allows us to investigate high-pressure phase transitions under nonhydrostatic conditions, in particular, the transition pressure and the enthalpy barrier, which are both decreasing if the pressure component along the c axis is larger than the other ones. Our results show an excellent agreement with available experimental and theoretical data. This enthalpy extraction method can also be extended to other phase transitions and to ones including orthorhombic structures, for example, the transitions β-tin$\rightarrow$*Imma*$\rightarrow$sh. Thus, we have developed a powerful tool for investigating phase transitions under hydrostatic and nonhydrostatic conditions.

ACKNOWLEDGMENTS

Support by the Heinrich Böll Stiftung, Germany, is gratefully acknowledged. K.G.-N. also likes to acknowledge G. Onida for discussions and carefully reading the manuscript. This work was funded, in part, by the EU's 6th Framework Programme through the NANOQUANTA Network of Excellence (Grant No. NMP4-CT-2004-500198).

APPENDIX: CALCULATION OF THE ENTHALPY INCLUDING STRESS

Here we give a short description of the formulas used for the calculation of the enthalpy, including stress and strain effects considering Eq. (5). In particular, we derive a formula to integrate

$$\mathrm{d}H = \mathrm{d}E - V_0 \sum_{j=x,y,z} \sigma_j \mathrm{d}\epsilon_j. \tag{A1}$$

Under hydrostatic conditions the enthalpy is

$$H = E + pV = E + V_0 p \frac{V - V_0}{V_0} + pV_0. \tag{A2}$$

The second term corresponds to the stress-strain term of Eq. (5) multiplied by V_0. Thus, considering Eqs. (4) and (5), the enthalpy can be written as

$$H = E + V_0 \sum_{j=x,y,z} p_j \frac{x_j' - x_j}{x_j} + p_0 V_0 = E - V_0 \sum_{j=x,y,z} \sigma_j \epsilon_j + p_0 V_0. \tag{A3}$$

Here the average pressure p_0 is used because the pressure p is not well defined in the nonhydrostatic case. Since Eq. (4) holds just for small stress, the integration is performed using the recursively defined equation

$$H^i = H^{i-1} + (E^i_{\mathrm{nh}} - E^{i-1}_{\mathrm{nh}}) + V^{i-1} \sum_{j=x,y,z} \frac{x^i_j - x^{i-1}_j}{x^{i-1}_j} p^i_j + V^{i-1}(p^i_0 - p^{i-1}_0) \tag{A4}$$

where x_j are the lattice constants along the three Cartesian directions x, y, and z, and the difference from the previous step $(i-1)$ is calculated along a line $p_x - p_z = d$ for fixed nonhydrostatic conditions (see Fig. 3), starting from the equilibrium structure of the cd phase. E_{nh} is here the total energy along a line $p_x - p_z = d$. The last term corresponds to the $p_0 V_0$ term in Eq. (A3) including a correction because of double counting. The enthalpy $H(p_0)$ under nonhydrostatic conditions with $p_0 = p_0(p_x, p_y, p_z)$ corresponds to the calculated points H^i. By symmetrizing this equation numerical errors have been reduced.

*Electronic address: katalin.gaal-nagy@physik.uni-regensburg.de

[1] M. I. McMahon and R. J. Nelmes, Phys. Rev. B **47**, R8337 (1993).
[2] M. I. McMahon, R. J. Nelmes, N. G. Wright, and D. R. Allan, Phys. Rev. B **50**, 739 (1994).
[3] J. Z. Hu, L. D. Merkle, C. S. Menoni, and I. L. Spain, Phys. Rev. B **34**, 4679 (1986).
[4] G. A. Voronin, C. Pantea, T. W. Zerda, L. Wang, and Y. Zhao, Phys. Rev. B **68**, 020102(R) (2003).
[5] Y.-X. Zhao, F. Buehler, J. R. Sites, and I. L. Spain, Solid State Commun. **59**, 679 (1986).
[6] H. Olijnyk, S. K. Sikka, and W. B. Holzapfel, Phys. Lett. **103A**, 137 (1984).
[7] A. Werner, J. A. Sanjurjo, and M. Cardona, Solid State Commun. **44**, 155 (1982).
[8] C. S. Menoni, J. Z. Hu, and I. L. Spain, Phys. Rev. B **34**, 362 (1986).
[9] A. Yoshiasa, K. Koto, H. Maeda, and T. Ishii, Jpn. J. Appl. Phys., Part 1 **36**, 781 (1997).
[10] I. L. Spain, J. Z. Hu, C. S. Menoni, and D. Black, J. Phys. (Paris) **45**, C8 (1984).
[11] A. D. Cicco, A. C. Frasini, M. Minicucci, E. Principi, J.-P. Itié, and P. Munsch, Phys. Status Solidi B **240**, 19 (2003).
[12] R. H. Wentorf and J. S. Kasper, Science **139**, 338 (1963).
[13] J. C. Jamieson, Science **139**, 762 (1963).
[14] K. Asaumi and S. Minomura, J. Phys. Soc. Jpn. **45**, 1061 (1978).
[15] T. I. Dyuzheva, S. S. Kabalkina, and V. P. Novichkov, Sov. Phys. JETP **47**, 931 (1978).
[16] M. C. Gupta and A. L. Ruoff, J. Appl. Phys. **51**, 1072 (1980).
[17] M. A. Baublitz and A. L. Ruoff, J. Appl. Phys. **53**, 5669 (1982).
[18] C. S. Menoni, J. Z. Hu, and I. L. Spain, in *High Pressure in Science and Technology*, edited by C. Homan, R. K. MacCrone, and E. Walley (North-Holland, Amsterdam, 1983).
[19] S. B. Quadri, E. F. Skelton, and A. W. Webb, J. Appl. Phys. **54**, 3609 (1983).
[20] J. Z. Hu and I. L. Spain, Solid State Commun. **51**, 263 (1984).
[21] E. Y. Tonkov, *High Pressure Phase Transformations* (Gordon and Breach Science Publishers, Philadelphia, 1992) Vol. 2.
[22] M. Hebbache and M. Zemzemi, Phys. Rev. B **67**, 233302 (2003).
[23] Y. K. Vohra, K. E. Brister, S. Desgreniers, A. L. Ruoff, K. J.

Chang, and M. L. Cohen, Phys. Rev. Lett. **56**, 1944 (1986).
[24] M. T. Yin and M. L. Cohen, Phys. Rev. Lett. **45**, 1004 (1980).
[25] M. T. Yin and M. L. Cohen, Solid State Commun. **38**, 625 (1980).
[26] M. T. Yin and M. L. Cohen, Phys. Rev. B **26**, 5668 (1982).
[27] M. T. Yin and M. L. Cohen, Phys. Rev. B **26**, 3259 (1982).
[28] R. J. Needs and R. M. Martin, Phys. Rev. B **30**, R5390 (1984).
[29] K. J. Chang and M. L. Cohen, Phys. Rev. B **30**, R5376 (1984).
[30] K. J. Chang and M. L. Cohen, Phys. Rev. B **34**, 8581 (1986).
[31] M. Methfessel, C. O. Rodriguez, and O. K. Andersen, Phys. Rev. B **40**, R2009 (1989).
[32] L. L. Boyer, E. Kaxiras, J. L. Feldman, J. Q. Broughton, and M. J. Mehl, Phys. Rev. Lett. **67**, 715 (1991).
[33] K. Mizushima, S. Yip, and E. Kaxiras, Phys. Rev. B **50**, 14952 (1994).
[34] R. J. Needs and A. Mujica, Phys. Rev. B **51**, 9652 (1995).
[35] N. Moll, M. Bockstedte, M. Fuchs, E. Pehlke, and M. Scheffler, Phys. Rev. B **52**, 2550 (1995).
[36] A. DalCorso, A. Pasquarello, A. Baldereschi, and R. Car, Phys. Rev. B **53**, 1180 (1996).
[37] B. G. Pfrommer, M. Côté, S. G. Louie, and M. L. Cohen, Phys. Rev. B **56**, 6662 (1997).
[38] I.-H. Lee and R. M. Martin, Phys. Rev. B **56**, 7197 (1997).
[39] N. E. Christensen, D. L. Novikov, R. E. Alonso, and C. O. Rodriguez, Phys. Status Solidi B **211**, 5 (1999).
[40] K. Gaál-Nagy, A. Bauer, M. Schmitt, K. Karch, P. Pavone, and D. Strauch, Phys. Status Solidi B **211**, 275 (1999).
[41] G. J. Ackland, Rep. Prog. Phys. **64**, 483 (2001).
[42] M. Hebbache, M. Mattesini, and J. Szeftel, Phys. Rev. B **63**, 205201 (2001).
[43] K. Gaál-Nagy, M. Schmitt, P. Pavone, and D. Strauch, Comput. Mater. Sci. **22**, 49 (2001).
[44] A. Mujica, A. Rubio, A. Muños, and R. J. Needs, Rev. Mod. Phys. **75**, 863 (2003).
[45] K. Gaál-Nagy, A. Bauer, P. Pavone, and D. Strauch, Comput. Mater. Sci. **30**, 1 (2004).
[46] K. Gaál-Nagy, P. Pavone, and D. Strauch, Phys. Rev. B **69**, 134112 (2004).
[47] M. Kaczmarski, O. N. Bedoya-Martínez, and E. R. Hernández, Phys. Rev. Lett. **94**, 095701 (2005).
[48] R. Biswas, R. M. Martin, R. J. Needs, and O. H. Nielsen, Phys. Rev. B **30**, 3210 (1984).
[49] R. Biswas, R. M. Martin, R. J. Needs, and O. H. Nielsen, Phys. Rev. B **35**, 9559 (1987).
[50] G. J. Piermarini, S. Block, and J. S. Barnett, J. Appl. Phys. **44**, 5377 (1973).
[51] J. S. Barnett, S. Block, and G. J. Piermarini, Rev. Sci. Instrum. **44**, 1 (1973).
[52] K. E. Brister, Y. K. Vohra, and A. L. Ruoff, Rev. Sci. Instrum. **59**, 318 (1988).
[53] C. Cheng, W. H. Huang, and H. J. Li, Phys. Rev. B **63**, R153202 (2001).
[54] C. Cheng, Phys. Rev. B **67**, 134109 (2003).
[55] J. F. Nye, *Physical Properties of Crystals* (Oxford University Press, London, 1969).
[56] P. M. Chaikin and T. C. Lubensky, *Principles of Condensed Matter Physics* (Cambridge University Press, Cambridge, England, 1995).
[57] L. D. Landau and E. M. Lifshitz, *Theory of Elasticity* (Pergamon Press, Oxford, 1970), Vol. VII.
[58] G. Kresse and J. Hafner, Phys. Rev. B **47**, R558 (1993).
[59] G. Kresse and J. Furthmüller, Phys. Rev. B **54**, 11169 (1996).
[60] G. Kresse, Ph.D. thesis, Technische Universität Wien (unpublished).
[61] G. Kresse and J. Furthmüller, Comput. Mater. Sci. **6**, 15 (1996).
[62] P. Hohenberg and W. Kohn, Phys. Rev. **136B**, 864 (1964).
[63] W. Kohn and L. J. Sham, Phys. Rev. **140A**, 1133 (1965).
[64] D. Vanderbilt, Phys. Rev. B **41**, R7892 (1990).
[65] G. Kresse and J. Hafner, J. Phys.: Condens. Matter **6**, 8245 (1994).
[66] J. P. Perdew, J. A. Chevary, S. H. Vosko, K. A. Jackson, M. R. Pederson, D. J. Singh, and C. Fiolhais, Phys. Rev. B **46**, 6671 (1992).
[67] J. P. Perdew and A. Zunger, Phys. Rev. B **23**, 5048 (1981).
[68] D. M. Ceperley and B. J. Alder, Phys. Rev. Lett. **45**, 566 (1980).
[69] S. Goedecker and K. Maschke, Phys. Rev. B **45**, 1597 (1992).
[70] R. P. Feynman, Phys. Rev. **56**, 340 (1939).
[71] P. Pulay, Mol. Phys. **17**, 197 (1969).
[72] H. J. Monkhorst and J. D. Pack, Phys. Rev. B **13**, 5188 (1976).
[73] M. Methfessel and A. T. Paxton, Phys. Rev. B **40**, 3616 (1989).
[74] I.-H. Lee, J.-W. Jeong, and K. J. Chang, Phys. Rev. B **55**, 5689 (1997).
[75] J. Wang, S. Yip, S. R. Phillpot, and D. Wolf, Phys. Rev. Lett. **71**, 4182 (1993).
[76] J. Wang, J. Li, S. Yip, S. Phillpot, and D. Wolf, Phys. Rev. B **52**, 12627 (1995).
[77] H. Libotte and J.-P. Gaspard, Phys. Rev. B **62**, R7110 (2000).
[78] M. Durandurdu, Phys. Rev. B **71**, 054112 (2005).
[79] K. Gaál-Nagy, Ph.D. thesis, Universität Regensburg, 2004.